NRIAG JOURNAL OF ASTRONOMY AND GEOPHYSICS
2022, VOL. 11, NO. 1, 113–119
https://doi.org/10.1080/20909977.2021.2000267

Derived precipitable water vapour from GNSS and radiosonde data using time series and spatial least-square

M. A. Abdelfatah[a], N. M. Elhaty[a], A. E. Mousa[b] and G. S. El-Fiky[a]

[a]Construction Department & Utilities, Faculty of Engineering, Zagazig University, Zagazig, Egypt; [b]National Research Institute of Astronomy and Geophysics, Helwan, Egypt

ABSTRACT

Precipitable water vapour (PWV) plays an important role in rain prediction; up to now, lots of different measuring methods and devices are developed to observe PWV. In this paper, radiosonde techniques are used to compute PWV's spatial and temporal variations and GNSS (Global Navigation Satellite Systems) using in spatial only. GNSS data (GPS and GLONASS) from eight Egyptian stations were processed for the year 2014. Five radiosonde stations for the period from 2005 to 2016 were used. Time series is constructed using the daily surface measurements of radiosonde stations. The linear trend is estimated by straight line fit over 12 years of seasonally adjusted PWV time series. The PWV in Egypt has a positive trend in time series at more than five radiosonde sites with a rate of 0.3 mm/year. The monthly cycle is a near sine curve and the stochastic errors are from 0% to 5.4% over 12 years. The comparison between PWV estimated from GNSS data using the PPP approach and radiosonde data for each station in year 2014 was done in the near station. The nearest two stations, GNSS station "MTRH" and radiosonde station "62,306", get a bias of 0.66 mm. Three common interpolation techniques (Inverse Distance Weighting, Kriging, and Minimum Curve) are used. The biases of the three used methods were 1.65 mm, 1.96 mm and 0.61 mm, respectively. The statistical methods of Minimum Curve interpolation are found superior to other methods with mean error at Mersa-Matrouh, Aswan and Al-Arish stations reaching 0.1 mm, 1.0 mm and 0.30 mm, respectively. The minimum curve technique is recommended in spatial interpolation for the prediction of PWV amount.

Abbreviations: PWV: precipitable water vapour; PPP: precise point positioning; GNSS: global navigation satellite system; ZPD: tropospheric zenith path delay; ZWD: zenith wet delay; IDW: inverse distance weighting; MC: minimum curvature; IGS: International GNSS service.

ARTICLE HISTORY
Received 15 August 2021
Revised 16 October 2021
Accepted 26 October 2021

KEYWORDS
Precipitable water vapour; radiosonde; GNSS; time series and spatial least square

1. Introduction

GNSS data obtained from ground-based stations started to offer an alternative image of the distribution of the vertically integrated water vapour PWV (Abdelfatah et al. 2019). GNSS information was found to contribute to atmospheric analysis for weather forecast (Sleem et al. 2019). The GNSS can estimate the tropospheric delay with high reliability of measurements (Li et al. 2015). The GNSS data processing increases the observations of satellite number throughout the atmosphere, improving the geometry, the time of processing, the redundancy and consequently the robustness of the PWV measurements (Benevides et al. 2015).

Time series analysis is very important as it provides information about the long-term behaviour (trend), the regular and periodic fluctuation (seasonal, cyclic) and irregular components of the studied phenomenon (stochastic) (Acheampong and Obeng 2019). Here, time series analysis is applied to study the PWV temporal variations.

PWV time series has different temporal variations that can be reasonably modelled using time series. Here, the following model (Alshawaf et al. 2017) is used, such that the time series of PWV_t can be expressed as

$$PWV_t = T_t * S_t * I_t \quad (1)$$

where T_t is the deterministic trend component, S_t is the seasonal component (e.g. periodicity = 12 months for PWV) and I_t is the irregular (stationary) stochastic component (Elhaty et al. 2019).

Here, there is no cyclic time series, which is known as seasonal adjustment (Alshawaf et al. 2017). The depersonalised data are useful for forecasting the PWV trend and estimating the irregular component is measured as no regular signal lasts longer than 1 year. The research procedure can be stated as

(1) Transforming wet tropospheric delay from GNSS to PWV: The technology regarding the ZPD (tropospheric zenith path delay)

CONTACT M. A. Abdelfatah m_amin2005@yahoo.com Faculty of Engineering, Zagazig University, Zagazig, Egypt

discernment was received abroad at the use of the unique factor positioning (PPP) job by means of The Canadian Geodetic Survey over Natural Resources modernised CSRS-PPP situation page. From ZPD, ZWD (zenith wet delay) may stay arrived by the way of subtracting ZHD (zenith hydrostat delay) from ZPD (Elhaty et al. 2019).

$$\mathrm{PWV} = \Pi * \mathrm{ZWD} \tag{2}$$

$$\Pi = 10^{-6}\rho \mathrm{R}_v\left(\frac{\mathrm{K}_3}{\mathrm{T}_\mathrm{m}} + \mathrm{K}_2^{'}\right) \tag{3}$$

$$\mathrm{T}_\mathrm{m} = 0.73\ \mathrm{T}_\mathrm{S} + 69.68 \tag{4}$$

where $\mathbf{K}_2^{'}$= (17 ±10) K $\mathbf{mb}^{-1}$, $\mathbf{K}_3$ = (3.776 ± 0.014) * 105 K $\mathbf{mb}^{-1}$. ρ is the thickness on the melted water, R_v is the specific fuel regular regarding water vapour, T_m is the weighted mean temperature, T_S is the surface temperature and Π is a conversion factor.

(1) Radiosonde and GNSS bias estimation for six nearest stations.
(2) Decomposing the time series method to obtain a trend, a seasonal and an irregular component of PWV from radiosonde data.
(3) Using the least square analyses to study the spatial variation of PWV over Egypt along 1 year using GNSS and radiosonde data.

2. Data collection

GNSS data from eight Egyptian stations were processed for the year 2014. These data were taken from the National Research Institute of Astronomy and Geophysics permanent network.

Five radiosonde stations were used from the Department of Atmospheric Science of the University of Wyoming which has a radiosonde database for the whole World from 2005 to 2016. These data were available at http://weather.uwyo.edu/upperair/sounding.html. The locations of the GNSS and radiosonde stations used are depicted in Figure 1.

3. Spatial variations of PWV

Long-term PWV time series from balloon soundings (radiosonde) integrated through the atmosphere can be investigated for climate analysis, particularly when they show agreement with the GNSS data.

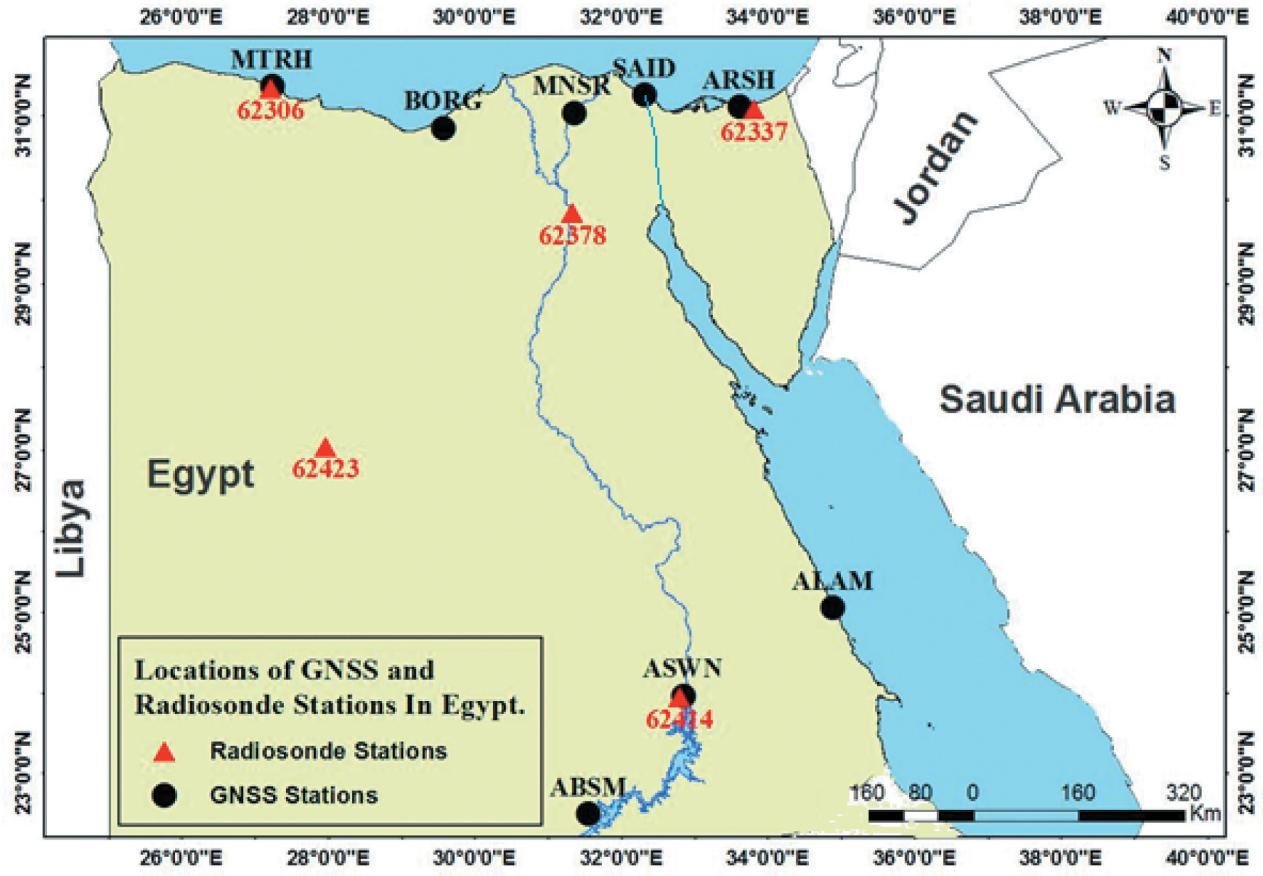

Figure 1. The locations of the GNSS and radiosonde stations used in this study.

Techniques of spatial interpolation were used to compute the PWV at a position within an unobserved station based on the application of known PWV from surrounding stations (Addink 1999). The general formula for spatial interpolation is as follows:

$$PWV_g = \sum_{i=1}^{n_s} w_i * PWV_{si} \quad (3)$$

where PWV_g is the interpolated (predicted) value of precipitable water vapour at point g, PWV_{si} is the observed value (sample points) at point i, ns is the total number of observed points and w_i is the weight at point i.

The main difference among interpolations techniques are in estimating the weights from the grid node. Some techniques, such as Inverse Distance Weighting (IDW), Kriging, and Minimum Curvature (MC), are often used in the spatial interpolation (Teegavarapu and Chandramouli 2005).

IDW is defined as a distance reverse function of each point from near points (Lu and Wong 2008). However, the Kriging method is a stochastic approach that generates a continuous surface that does not pass through all sample points. The estimation provided by it is an unbiased compute of the observed value with the minimum variance (Ly and Degr´e 2011). The MC method is a fitting surface to a linearly elastic plate passing through each of the observed values with a minimum amount of bending (Yang et al. 2006).

For accurate selection of the PWV from GNSS, the PWV was compared from the GNSS and radiosonde data using ten stations with the other three GNSS stations that are used as reference stations. The above three-interpolation techniques are used to derive values on locations where no measurements are taken from the surrounding radiosonde and GNSS stations.

4. Results and discussion

4.1. Time series from radiosonde stations

4.1.1. Estimating the trend using least squares regression

The mean values and annual amplitudes of the PWV were determined for the period from 2005–2016 at five radiosonde sites in Egypt. The mean values of the PWV at northern region stations (Mersa-Matrouh and Al-Arish) are in the range of 15.9–20.3 mm, mostly larger than those in other regions. For the mid station (Helwan), the PWV found to be in the range of 12.5–15.9 mm, but this value at the southern region stations (Aswan and Farafra) ranges from about 12.5–14.9 mm. so, it can be said that the values of water vapour vary with the location of the station.

The obtained trends along with their precision from the above mentioned five radiosonde stations for 12 years of data time periods are show in Figure 2. The results show that there are some differences in the PWV magnitudes.

To verify the obtained tends, Figure 3 shows the time series residual of the PWV annual variations from 2005 to 2016 at the five radiosonde stations. The figure indicates the residual of scattering data against trend. The results show that the maximum error reaches 3.39 mm at station 62,337 in 2012.

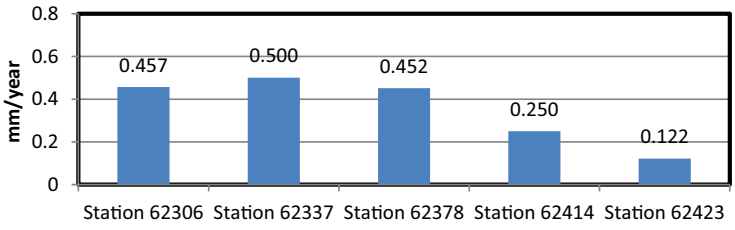

Figure 2. The estimated trends for different sites of PWV time series.

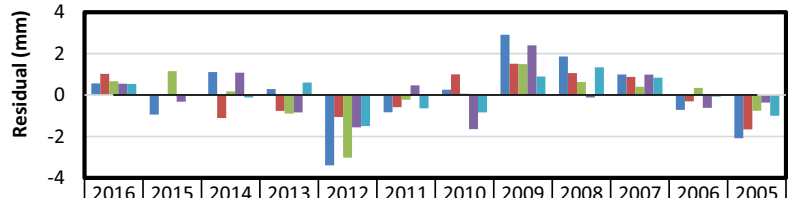

	2016	2015	2014	2013	2012	2011	2010	2009	2008	2007	2006	2005
62337	0.56	-0.95	1.11	0.29	-3.39	-0.84	0.26	2.91	1.86	0.99	-0.72	-2.09
62423	1.02	0.02	-1.11	-0.76	-1.06	-0.59	1.00	1.51	1.06	0.88	-0.30	-1.66
62414	0.67	1.15	0.18	-0.90	-3.03	-0.23	0.06	1.49	0.63	0.40	0.34	-0.76
62306	0.55	-0.32	1.08	-0.84	-1.56	0.47	-1.65	2.40	-0.12	0.99	-0.62	-0.37
62378	0.53	-0.03	-0.12	0.60	-1.50	-0.64	-0.84	0.89	1.34	0.84	-0.07	-1.00

Figure 3. Time series residual of the PWV annual variations from 2005 to 2016 at the five radiosonde stations.

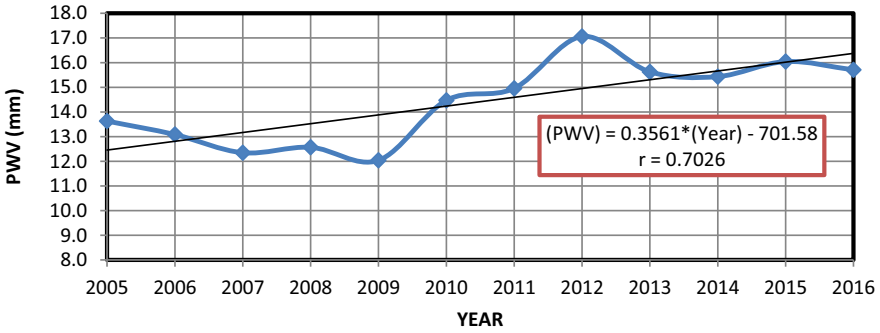

Figure 4. Annual trend variations of PWV.

On the other hand, the regional trends for the above five stations were computed from the mean daily time series. Figure 4 shows the trend of mean PWV level over Egypt. PWV increased temporarily during 2005–2016 with a trend of 0.3 mm/year.

4.1.2. Estimated monthly cycle

Figure 5 shows the monthly percentage averages (S_t) of PWV at two epochs (00–00 and 00–12-18 UTC) of each day for the whole period 2005–2016 for all the five sites. The percentages of the absolute values of PWV are under 0.5 mm from radiosonde data. Moreover, the variation of water vapour content is higher in the summer months than the winter months, which reflect the transition from dry to wet season at these geographical locations.

4.1.3. Stochastic time series

Figure 6 illustrates the 12-year stochastic error (I_t). The error was less than 1% during the 4 years (2015, 2013, 2011 and 2006), while the maximum error was 5.4% in 2012, which gives good confidence in the trend.

4.2. Radiosonde and GNSS bias estimation

Three GNSS stations "ASRH, ASWN and MTRH" were selected near the three other radiosonde station "62,337, 62,414 and 62,306" with 18, 7 and 2.6 km, respectively, see Figure 1. A 1-year data set (2014) was used for both techniques. The PPP technique was adopted to estimate ZTD, which were converted to GPS-PWV by using one key parameters "T_m". The results indicate that GNSS data can be used for tropospheric delay monitoring with high accuracy (MTRH bias of 0.66 mm). This can be achieved by using PPP (see Figure 7).

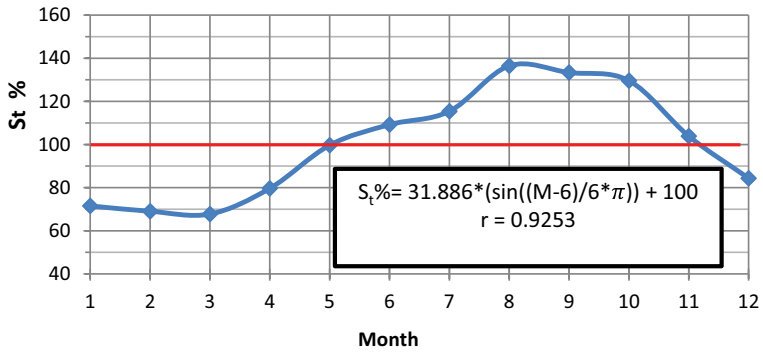

Figure 5. Mean monthly percentage average of PWV (%) from 2005 to 2016 for the five-radiosonde station.

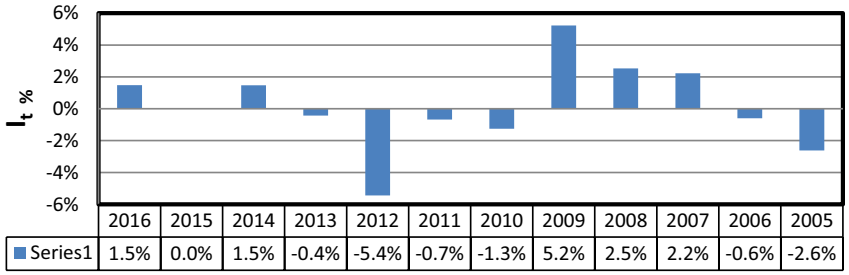

Figure 6. Percentage average of PWV (%) stochastic error from 2005 to 2016 for the five radiosonde stations.

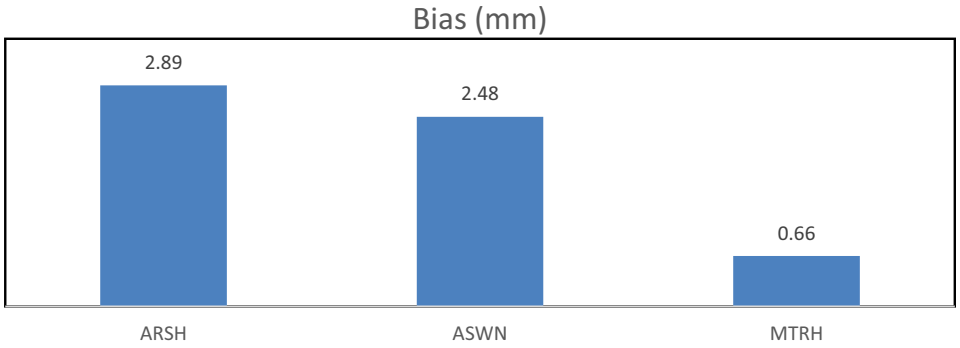

Figure 7. PWV stations bias from GNSS and radiosonde data in Egypt (2014).

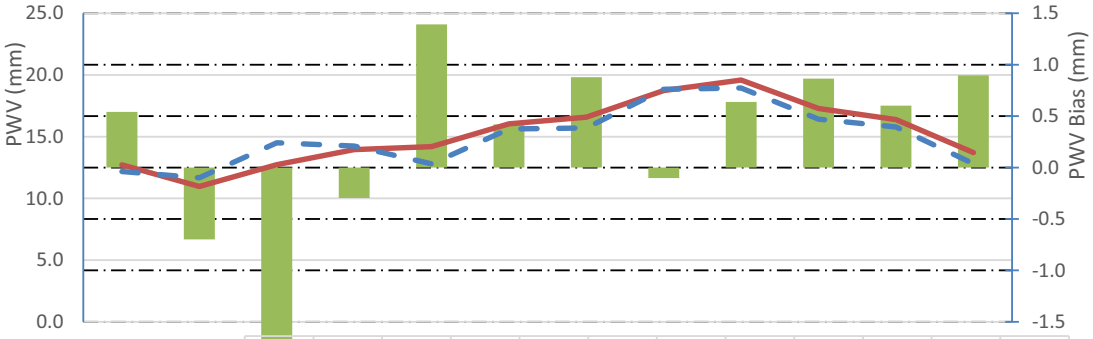

	Jan-14	Feb-14	Mar-14	Apr-14	May-14	Jun-14	Jul-14	Aug-14	Sep-14	Oct-14	Nov-14	Dec-14
Bias	0.5	-0.7	-1.8	-0.3	1.4	0.4	0.9	-0.1	0.6	0.9	0.6	0.9
PWV from RS	12.7	11.0	12.7	13.9	14.2	16.0	16.6	18.7	19.6	17.3	16.4	13.7
PWV from GNSS	12.2	11.7	14.5	14.2	12.8	15.6	15.7	18.8	18.9	16.4	15.8	12.8

Figure 8. PWV monthly bias from GNSS and radiosonde data in Egypt (2014).

Figure 8 illustrates comparison between average PWV time series estimated from GNSS data and radiosonde data.

This effort is intended to computing the PWV improving both the spatial and temporal resolutions required for estimating the PW in this country, to help for developing accurate weather prediction and global climate models and to fill the observation Data gaps and knowledge related to water vapour contrast in this part of the world for the first time.

4.3. Spatial variations of PWV

Long-time series of PWV values from balloon soundings integrated through the atmosphere can be investigated for climate analysis, particularly when they show sufficient agreement with the GNSS data (GPS and GLONASS). The data used for studying the interpolation techniques are 13 GNSS and radiosonde stations over year 2014. Ten out of the 13 stations were used for building the model, while the other three were used for testing the obtained model.

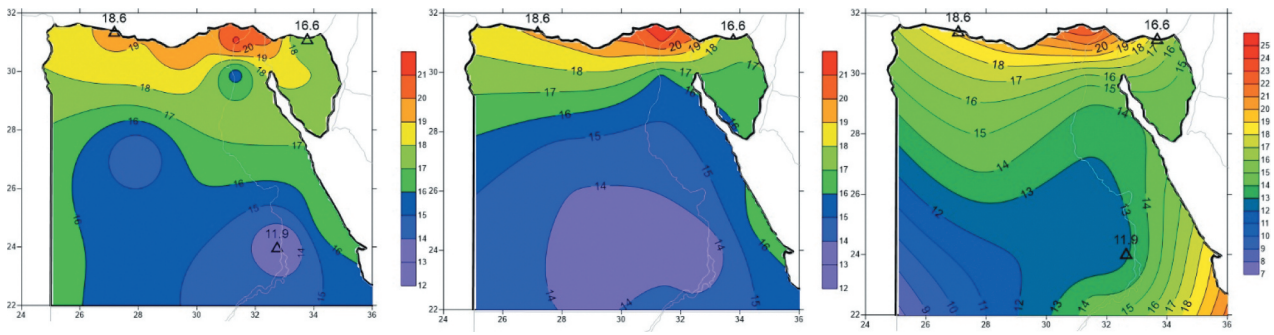

Figure 9. PWV map for Egypt using interpolation technique. Unit is mm. (a) IDW technique, (b) Kringing technique and (c) MC technique.

Figure 9(a) shows the PWV distribution maps generated by inverse distance weighting (IDW) technique. Clearly from this figure, the max value of PWV is found in the northern part of Egypt and reached about 21 mm. The estimated mean error by this technique for Mersa-Matrouh, Aswan and Al-Arish stations reached 1.5 mm, 2.0 mm and 1.4 mm, respectively.

The prediction biases were validated using the differences between the Kringing predicted values and the measured values at these sample points because the latter can be assumed as the truth. Figure 9(b) shows the PWV distribution maps generated by Kringing technique. It is easily seen from this figure that, the max value of PWV reached about 22 mm in the northern part of Egypt. The estimated mean error by this technique for Mersa-Matrouh, Aswan and Al-Arish stations found to be 1.5 mm, 2.0 mm and 2.3 mm, respectively.

The PWV distribution using minimum curvature (MC) technique is presented in Figure 9(c). This map confirmed that the value of PWV is higher in the northern part than southern part of Egypt. The mean error of the present technique for Mersa-Matrouh, Aswan and Al-Arish stations reached 0.10 mm, 1.0 mm and 0.30 mm, respectively.

The results indicate that the value of PWV is higher in the northern part than southern part of Egypt. The performance of the Minimum Curve technique was superior to inverse distance weighting and Kriging.

5. Conclusion

PWV time series determined the daily surface measurements of radiosondes stations and trend component, a seasonal component and a stochastic irregular component has been estimated. To evaluate the temporal evolution of PWV, the time series component have been deterministic modelled. Regional trends were computed from the yearly time series for each radiosonde station. The least squares fit for the trend has been computed with equal weighting for each estimated mean regional PWV value for each region. A positive trend in the PWV content with an increase of 0.30 mm/year has been found. In addition, the linear trend coefficients at each meteorological station have been estimated. Although PWV is high temporal variation, the calculated trend can be used to predict PWV using seasonal and stochastic components.

It has been demonstrated that GNSS technique has the potential to measure column abundance of water vapour, where the result shows that there is very good agreement between the PWV amounts estimated from GNSS signal delay measurements and those derived from radiosondes data. With biases 2.89, 2.48 and 0.66 mm for GNSS station ARSH, ASWN and MTRH, respectively, comparisons between the PWV values derived from GNSS data and radiosonde data were performed. The same atmospheric parameters were used to achieve advantageous when comparing different instruments. Finally, spatial interpolation technique has been used to obtain the PWV at a position within an unmeasured area. The performance of the minimum curvature technique is superior to other techniques. The minimum curvature technique could reach biases equal 0.1 mm.

Acknowledgements

The contribution of data from the department of atmospheric science of the University of Wyoming is appreciated.

Disclosure statement

No potential conflict of interest was reported by the author(s).

Funding

This research was funded by the authors.

Authors' contributions

Abdelfatah conceived and designed the experiments. Abdelfatah and Elhaty performed the experiments, analyzed the data and wrote the paper. Abdelfatah, Mousa and ElFieky reviewed the paper. All authors read and approved the final manuscript.

Availability of data and materials

All data in this paper are online at http:/weather.uwyo.edu/upperair/sounding.html

Ethics

Approval

References

Abdelfatah MA, Elhaty NM, Mousa AE, El-Fiky GS. 2019. Precipitable water vapor data derived from GNSS and radiosonde for Egypt. Cairo (Egypt): Civil Eng., Research Magazine (CERM), Faculty of Eng., Al-Azhar University.

Acheampong A, Obeng K. 2019. Application of GNSS derived precipitable water vapour prediction in West Africa. J Geod Sci. 9:41–47. doi:10.1515/jogs-2019-0005

Addink EA. 1999. Acoparison of conventional and geostatistical method to replace clouded pixels in NOAA-AVHRR image. Int J Remote Sens. 20:961–977. doi:10.1080/014311699213028.

Alshawaf F, Dick G, Heise S, Balidakis K, Schmidt T, Wickert J. 2017. Decadal variations in atmospheric water vapor time series estimated using GNSS. ERA-Interim, and synoptic data. In EGU General Ass. Conf. Abst. 19. p. 2721.

Benevides P, Nico G, Catalao J, Miranda PMA. 2015. Can Galileo increase the accuracy and spatial resolution of the 3D tropospheric water vapour reconstruction by GPS tomography? IEEE International Geoscience and Remote Sensing Symposium (IGARSS); July 26–31. p. 3603–3606 doi:10.1109/IGARSS.2015.7326601.

Elhaty NA, Mousa M, El-Fiky G. 2019 May. GNSS meteorology in Egypt: modeling weighted mean temperature from radiosonde data. Alexandria Eng J. 58:443–450. License CC BY-NC-ND 4.0. doi:10.1016/j.aej.2019.04.001

Li X, Dick G, Lu C, Ge M, Nilsson T, Ning T, Wickert J, Schuh H. 2015. Multi-GNSS meteorology: real-time retrieving of atmospheric water vapour from BeiDou, Galileo, GLONASS and GPS observations. IEEE T Geosci Remote. 53:6385–6393. doi:10.1109/TGRS.2015.2438395

Lu GY, Wong DW. 2008. An adaptive inverse-distance weighting spatial interpolation technique. Comput Geosci. 34:1044–1055. doi:10.1016/j.cageo.2007.07.010.

Ly SCC, Degr´e A. 2011. Geostatistical interpolation of daily rainfall at catchment scale: the use of several variogram models in the Ourthe and Ambleve catchments, Belgium. Hydrol Earth Syst Sci. 15:2259–2274. doi:10.5194/hess-15-2259-2011

Sleem RE, Abdelfatah M, Mousa A, El-Fiky G. 2019 September. Performance analysis of GNSS networks: a case study of the permanent network in Egypt. Int J Sci Eng Res. 10(9):1590.

Teegavarapu R, Chandramouli V. 2005. Improved weighting methods, deterministic and stochastic data-driven models for estimation of missing precipitation records. J Hydrol. 312:191–206. doi:10.1016/j.jhydrol.2005.02.015.

Yang C,S, Lee KF, Hung P. 2006. Twelve differentgInterpolation methods. “a case study of surfer 8.0, geo-imagery bridging continents”. XXth ISPRS Congress; 2004 July 12–23; Istanbul.